MAGNETOHYDRODYNAMICS Vol. 59 (2023), No. 3-4, pp. 265–280
DOI: 10.22364/mhd.59.3-4.2

MERGING OF ENSAMBLES OF ROTLETS

B. Shinde, A. Cēbers

MMML Lab, Faculty of Physics and Mathematics, University of Latvia, 3 Jelgavas str., Riga LV-1004, Latvia

We present a two-dimensional numerical simulation to study the behavior of two ensembles of rotlets. Initially, we examined a scenario in which the model was based solely on hydrodynamic interactions between particles. This preliminary analysis revealed that an ensemble of rotlets revolves around each other, similar to two rotlets rotating around a stable center of mass, and traces circular trajectories. This behavior was then compared with theoretical predictions. Subsequently, the repulsive forces were incorporated into the model. In this new system, two ensembles initially rotated around each other. Over time, they merge, which results in a single-ordered rotating structure. The eventual configuration obtained depends on the initial distance separating the ensembles, either a stable hexagonal ordered structure or a disordered structure, which is characterized by the hexatic order parameter.

Introduction. The mechanism of ordered structure formation via self-assembly has been extensively studied in different research fields [1]. In particular, magnetic soft matter has received great attention of researchers due to the observed ordered pattern in an ensemble of magnetized particles exposed to the external magnetic field. Ensembles of rotating magnetic droplets [2], the dynamics of self-assembly of magnetized disks [3, 4] have been studied experimentally and theoretically to understand the underlying mechanism for the ordered structure formation, dynamic and programmable self-assembly of micro-rafts [5], and rotating crystals of magnetic Janus colloidal particles [6] are some examples of self-assembly of spinners. In [2], an ensemble of magnetic droplets (micron size in diameter) was studied experimentally, where magnetic droplets formed a rotating structure with hexagonal order under an external rotating magnetic field. Because in [2](Fig. 2) experiments on several interacting ensembles of spinners were carried out, it would be interesting to study their evolution when hydrodynamic interactions and steric repulsion between particles are considered.

In this work, we study the behavior of two ensembles of rotlets and their merging in two parts: first, when only hydrodynamic interactions between particles are considered, and second, when along with hydrodynamic interactions, the steric repulsion between particles is also considered. In the first case, the ensembles follow circular trajectories; however, in the second case, the ensembles merge. After merging, the ensembles tend to form a single-ordered structure. Our findings have revealed that as the separation between the ensembles increases, the time needed for merging also increases, and, after merging, the system needs a considerable amount of time to reach a stable state. However, the initial separation between ensembles may not lead to the formation of an ordered structure. When the initial separation was minimal, the final structure exhibited a hexagonal arrangement.

1. Model.

We considered a two-dimensional (2D) ensemble of rotating particles. Each particle in the ensemble rotating with an angular velocity $\vec{\omega} = (0, 0, \omega)$ applies a torque $\vec{M}$ at its mass center, producing a flow around it. The velocity field generated by an individual

particle can be described as follows,

$$\vec{v}(\vec{r}) = \frac{[M\vec{e}_z \times \vec{r}]}{8\pi\eta|\vec{r}|^3}, \tag{1}$$

where $\vec{r}$ is the radius vector from the center of the spherical particle, η is the viscosity of the fluid. The particles in the ensemble interact owing to the flow field created by each particle; therefore, the motion of the i^{th} particle in the velocity field is calculated as the sum of the velocity fields produced by all other particles at the center of mass of the i^{th} particle. Thus, the equation of motion describing the dynamics of the i^{th} particle is

$$\frac{\mathrm{d}\vec{r}_i}{\mathrm{d}t} = \sum_{i\neq j} \frac{M[\vec{e}_z \times (\vec{r}_i - \vec{r}_j)]}{8\pi\eta|\vec{r}_i - \vec{r}_j|^3}. \tag{2}$$

Equation (2) may be written in Hamiltonian form by introducing $(x_i, p_i) = (x_i, y_i)$,

$$\dot{x}_i = \frac{\partial H}{\partial p_i}, \tag{3}$$

$$\dot{p}_i = -\frac{\partial H}{\partial x_i}, \tag{4}$$

$$H = \frac{1}{2}\sum_{i\neq j} \frac{1}{|\vec{r}_i - \vec{r}_j|}. \tag{5}$$

As H is an integral of motion, the rotlets cannot approach each other too closely. The second integral of motion $\sum_i (x_i^2 + y_i^2)$ resulting from the rotational invariance of the Hamiltonian implies that the rotlets are confined to a limited region of the plane. We then included the steric repulsion between the particles in the ensemble. The velocity induced by repulsive interactions reads as

$$\vec{v}_{\text{rep}}(\vec{r}_i - \vec{r}_j) = \sum_{i\neq j} L_0 \frac{(\vec{r}_i - \vec{r}_j)}{|\vec{r}_i - \vec{r}_j|} \mathrm{e}^{-\frac{|\vec{r}_i - \vec{r}_j|}{r_s}}, \tag{6}$$

where L_0 is the magnitude of the velocity induced by repulsion, and r_s is the range of repulsion and has dimensions of length. Adding the velocities Eq. (2) and Eq. (6), the equation of motion describing the dynamic of an ensemble consisting of N particles is written as

$$\frac{\mathrm{d}\vec{r}_i}{\mathrm{d}t} = \sum_{i\neq j} \frac{M[\vec{e}_z \times (\vec{r}_i - \vec{r}_j)]}{8\pi\eta|\vec{r}_i - \vec{r}_j|^3} + \sum_{i\neq j} L_0 \frac{(\vec{r}_i - \vec{r}_j)}{|\vec{r}_i - \vec{r}_j|} \mathrm{e}^{-\frac{|\vec{r}_i - \vec{r}_j|}{r_s}}. \tag{7}$$

The distance is scaled by a (the mean distance between particles) and the velocity by $v_h = M/(8\pi\eta a^2)$. When introducing dimensionless parameters $\vec{r}_i = \vec{r}_i/a$, $\tau = tv_h/a$, $\lambda = L_0/v_h$, $r_s = r_s/a$ (tilde is further omitted), where λ characterizes the ratio of velocity induced by repulsion and the characteristic velocity induced by hydrodynamic interactions, the equations of motion without repulsion and with repulsion written in the dimensionless form are, respectively,

$$\frac{\mathrm{d}\vec{r}_i}{\mathrm{d}\tau} = \sum_{i\neq j} \frac{\vec{e}_z \times (\vec{r}_i - \vec{r}_j)}{|\vec{r}_i - \vec{r}_j|^3}, \tag{8}$$

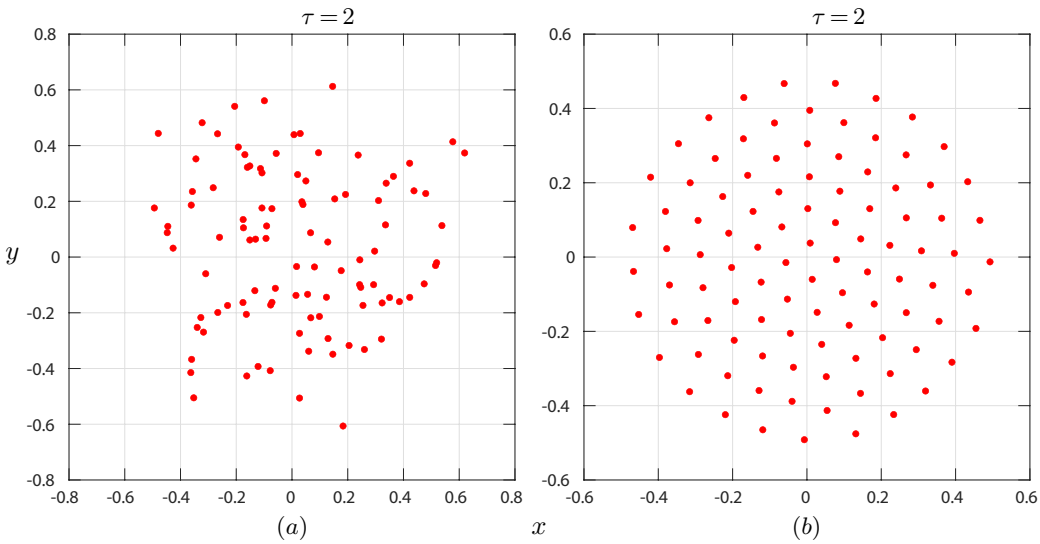

Fig. 1. The evolution of ensembles. (*a*) The ensemble remains disordered when only the hydrodynamic interaction is present, Eq. (8), shown for the time $\tau = 2$. (*b*) The ensemble reached an ordered state at the time $\tau = 2$ when repulsion was included along with the hydrodynamic interaction Eq. (9). The ensemble consisted of $N = 100$ rotlets with the parameters $\lambda = 0.2$ and $r_s = 0.05$. The x and y are the coordinates of the particle positions.

$$\frac{\mathrm{d}\vec{r}_i}{\mathrm{d}\tau} = \sum_{i \neq j} \frac{\vec{e}_z \times (\vec{r}_i - \vec{r}_j)}{|\vec{r}_i - \vec{r}_j|^3} + \sum_{i \neq j} \lambda \frac{(\vec{r}_i - \vec{r}_j)}{|\vec{r}_i - \vec{r}_j|} \mathrm{e}^{-\frac{|\vec{r}_i - \vec{r}_j|}{r_s}}, \tag{9}$$

where r_s and λ are the dimensionless parameters. Rotating particles in an ensemble exhibit a chaotic motion due to the hydrodynamic interactions, Eq. (8) and Fig. 1*a*. Adding repulsion causes the particles to reach an ordered state, where the hydrodynamic interactions are balanced, and the system evolves to a steady state, Eq. (9) and Fig. 1*b*.

2. Numerical simulation results.

2.1. Dynamics of two rotating ensembles without steric repulsion. In our previous work [8], we studied in detail the dynamics and evolution of single ensembles consisting of rotating particles. We observed that two particles in a large ensemble orbit each other with a fixed center of mass and trace a circular path when only hydrodynamic interactions between the particles were present. This motivated us to observe the dynamics of two rotating ensembles without and with steric repulsion. Thus, for hydrodynamic interactions only, instead of two rotating particles, we examined two ensembles of particles, each ensemble consisting of $N = 10$ particles that were initially separated by a distance of $d = 4$. Over time, the ensembles rotated around each other and followed a circular path. To determine the trajectory of each ensemble analytically, we assumed that the position of each ensemble is defined by a radius vector from its center of mass $\vec{R}_1$ for ensemble one, $\vec{R}_2$ for ensemble two, and $\vec{R} = \vec{R}_1 - \vec{R}_2$. Therefore, the motion of the radius vectors $\vec{R}_1$ and $\vec{R}_2$ is given approximately by equations in a dimensionless form as

$$\frac{\mathrm{d}\vec{R}_1}{\mathrm{d}\tau} = N \frac{[\vec{e}_z \times (\vec{R}_1 - \vec{R}_2)]}{|\vec{R}|^3}, \tag{10}$$

$$\frac{\mathrm{d}\vec{R}_2}{\mathrm{d}\tau} = N\frac{[\vec{e}_z \times (\vec{R}_2 - \vec{R}_1)]}{|\vec{R}|^3}, \tag{11}$$

where N is the total number of particles in each ensemble (the total number of particles in both ensembles is denoted as N_T). The center of mass for ensembles located at (0,0) $\vec{R}_1 + \vec{R}_2 = 0$, which implies $\vec{R}_1 = -\vec{R}_2$ using this condition, and Eq. (10) and Eq. (11) read

$$\frac{\mathrm{d}\vec{R}_1}{\mathrm{d}\tau} = 2N\frac{[\vec{e}_z \times \vec{R}_1]}{|\vec{R}|^3}, \tag{12}$$

$$\frac{\mathrm{d}\vec{R}_2}{\mathrm{d}\tau} = 2N\frac{[\vec{e}_z \times \vec{R}_2]}{|\vec{R}|^3}, \tag{13}$$

$$\frac{\mathrm{d}\vec{R}_1}{\mathrm{d}\tau} = 2N\frac{(-y_{\mathrm{cm}1}\hat{i} + x_{\mathrm{cm}1}\hat{j})}{|\vec{R}|^3}, \tag{14}$$

$$\frac{\mathrm{d}\vec{R}_2}{\mathrm{d}\tau} = 2N\frac{(-y_{\mathrm{cm}2}\hat{i} + x_{\mathrm{cm}2}\hat{j})}{|\vec{R}|^3}, \tag{15}$$

where $(x_{\mathrm{cm}1}, y_{\mathrm{cm}1})$ and $(x_{\mathrm{cm}2}, y_{\mathrm{cm}2})$ are the coordinates of the positions of the center of mass for ensemble one and ensemble two. The solution to Eq. (14), Eq. (15), respectively, is

$$\vec{R}_1 = \left(x_{\mathrm{cm}10}\cos(\omega\tau) - y_{\mathrm{cm}10}\sin(\omega\tau)\right)\hat{i} + \left(x_{\mathrm{cm}10}\sin(\omega\tau) + y_{\mathrm{cm}10}\cos(\omega\tau)\right)\hat{j}, \tag{16}$$

$$\vec{R}_2 = \left(x_{\mathrm{cm}20}\cos(\omega\tau) - y_{\mathrm{cm}20}\sin(\omega\tau)\right)\hat{i} + \left(x_{\mathrm{cm}20}\sin(\omega\tau) + y_{\mathrm{cm}20}\cos(\omega\tau)\right)\hat{j}, \tag{17}$$

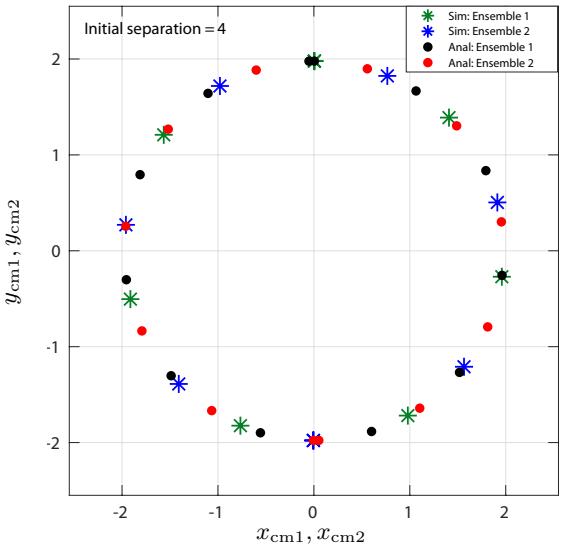

Fig. 2. Numerical simulation and analytical comparison of two ensembles rotating as two rotlets and following circular trajectories when only the hydrodynamic interaction between particles is present. This indicates a complete single rotation from $\tau = 0$ to $\tau = 19.6$. $\vec{R}_1 = (x_{\mathrm{cm}1}, y_{\mathrm{cm}1})$ is the center of mass of ensemble one, and $\vec{R}_2 = (x_{\mathrm{cm}2}, y_{\mathrm{cm}2})$ is the center of mass of ensemble two. For the simulation, green stars and blue stars are in anti-phase with each other, and for the analytical result, black and red particles are in anti-phase. $N = 10$ in each ensemble.

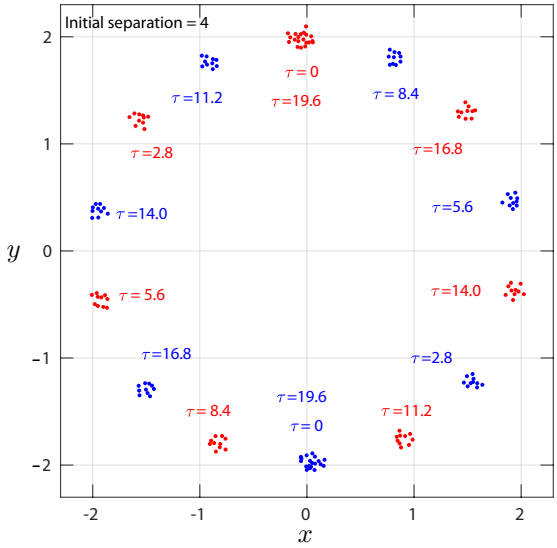

Fig. 3. Simulation of one complete rotation of two ensembles for the period $\tau = 19.6$ with different time steps that trace circular trajectories. The ensembles rotate at opposite positions on the diameter of the circular trajectory (in anti-phase): ensemble one (red) and ensemble two (blue). The x and y are the coordinates of the positions of the particles in each ensemble, and $N = 10$ in each ensemble.

where $\omega = 2N/|\vec{R}|^3$ is the angular frequency, $(x_{\mathrm{cm}10}, y_{\mathrm{cm}10})$ and $(x_{\mathrm{cm}20}, y_{\mathrm{cm}20})$ are the coordinates of the positions of the center of mass for ensemble one and ensemble two at the time $\tau = 0$, respectively. Fig. 2 illustrates a quantitative good match of the circular trajectories of the two rotating ensembles obtained by numerical simulation and analytical result. The trajectories are shown for one complete rotation by simulation (from $\tau = 0$ to $\tau = 19.6$), where green stars for ensemble one and blue stars for ensemble two, both are in anti-phase with each other, and from analytical results for ensembles one, Eq. (16), and two, Eq. (17), are shown in black and red particles, respectively, and are also in anti-phase with each other ($\vec{R}_1 = -\vec{R}_2$). The initial separation between the ensembles was $d = 4$. Fig. 3 shows the actual simulated rotation of the ensembles over time with a period of $\tau = 19.6$. Both ensembles are initially situated at opposite positions, indicated in red and blue, respectively, at $\tau = 0$, that is, in anti-phase. As time elapsed, the ensembles began to rotate around each other, as shown at different time steps. At each time step, both ensembles rotated at the opposite side of the diameter, and the corresponding time step was denoted by the same color as the ensembles.

Furthermore, when the two ensembles were spaced apart by a distance of one ($d = 1$) and again only the hydrodynamic interaction between the particles was considered, it was observed that these ensembles began rotating along a circular path and eventually merged. The resulting merged structure remained chaotic, as shown in Fig. 4. The trajectories calculated for both ensembles are presented in Fig. 5*a*, where it shows some number of rotation of the ensembles at the beginning. We can also see another concentric circular path, which was observed owing to the exchange of particles between

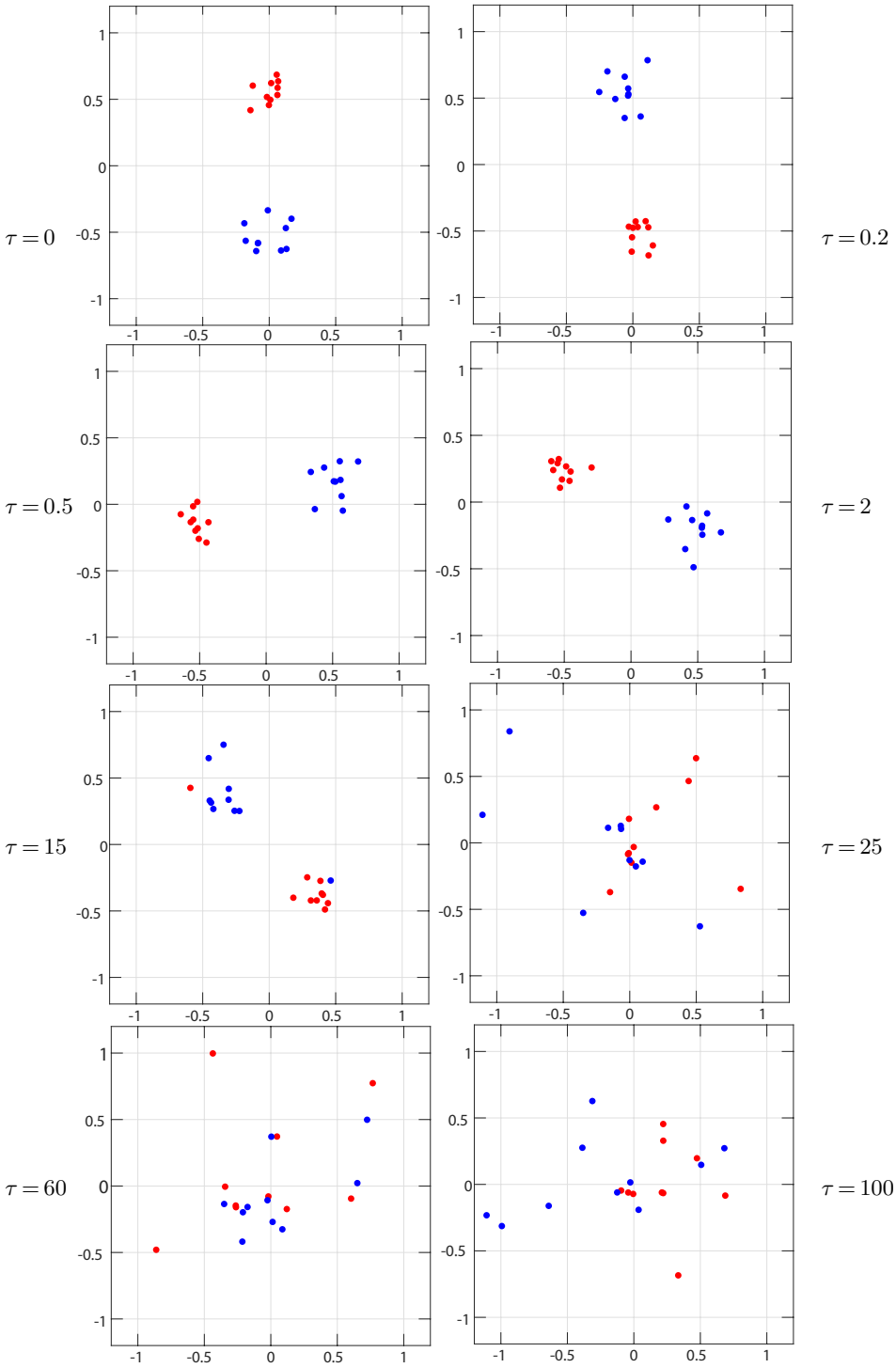

Fig. 4. Merging of ensembles when only the hydrodynamic interaction is present at $d = 1$ and $N = 10$ in each ensemble.

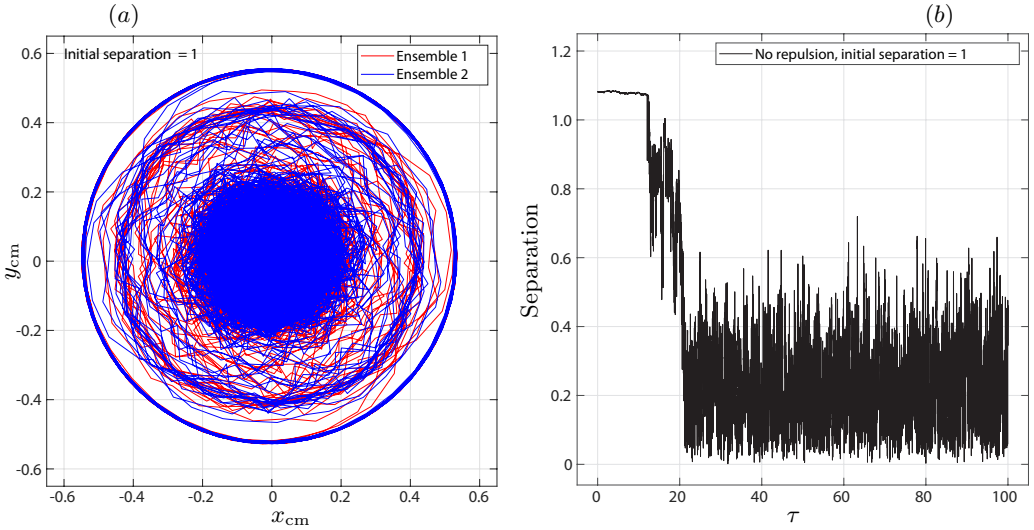

Fig. 5. (*a*) Trajectory of the center of mass of each ensembles. (*b*) Separation between the center of mass of two ensembles with time. Only hydrodynamic interactions between particles are present. The total number of particles in each ensemble is $N = 10$ and the initial separation between ensemble is $d = 1$.

the ensembles as the separation between them decreased (Fig. 4, $\tau = 15$) and later they get merged that shows chaotic trajectories at the center. The separation between the ensembles over time is shown in Fig. 5*b*, merging occurred around $\tau = 25$ and the further fluctuation in the separation is due to the chaotic motion of particles in the final ensemble.

2.2. Dynamics of two rotating ensembles with steric repulsion. It is fascinating to observe the dynamics of two ensembles of particles as they rotate around each other when repulsion is introduced between the particles. To gain insight into the final evolution of the two rotating ensembles at a late time τ, we conducted numerical simulations of Eq. (9) and analyzed their dynamics based on the different initial separation between the ensembles. Each particle moves through the velocity field generated by the other particles in the same ensemble as well as those in the second ensemble. A notable observation was made that the ensembles turned around each other, the distance between them reduced, and they merged into a single large ensemble over time owing to velocity fluctuations. The final state of the last single ensemble was determined to be either ordered or disordered based on the initial distance between the two ensembles and for the fixed parameter values (λ and r_s). At $\tau = 0$, the particles were uniformly distributed in a circle of radius 0.2 and constituted an ensemble. At $\tau = 0$, the position of the center of mass of ensemble one was at $\vec{R}_1$ and the position of the center of mass of ensemble two was at $\vec{R}_2$. The initial separation between the ensembles was given by $\vec{R}_1 - \vec{R}_2$. A similar initial configuration of the two ensembles was considered in further calculations. We analyzed the system with different initial separations between the two ensembles for $d = 1$, $d = 4$, and $d = 6$, while keeping the values of the parameters fixed at $\lambda = 0.5$ and $r_s = 0.05$ for a system with $N = 50$ particles in each ensemble. We then tracked the evolution of the system at different time steps τ, showing that the final state of the combined ensemble was either ordered or disordered.

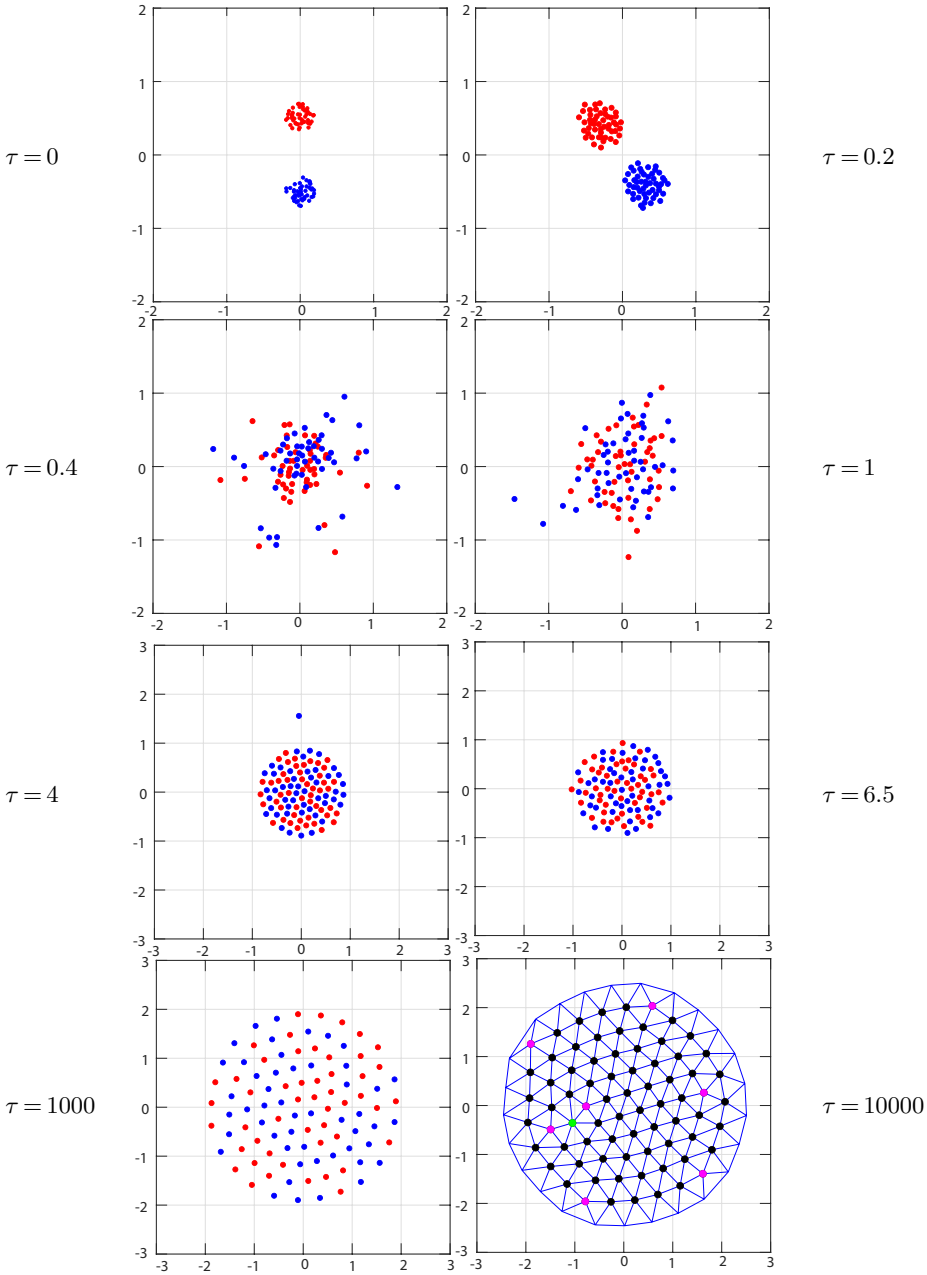

Fig. 6. Merging of two ensembles with time τ (red particles – ensemble one and blue particle – ensemble two), where the initial separation between the ensembles was $d = 1$, the parameters were $\lambda = 0.5$ and $r_s = 0.05$, the number of particles in each ensemble $N = 50$, and the total number of particles in the final single ensembles $N_{\mathrm{T}} = 100$. The system evolves to a steady state, where it forms a hexagonally ordered structure, as shown by the Delaunay triangulation at $\tau = 10000$, where black particles have six neighbors, pink particles have five neighbors, and green particles have seven neighbors. The pink and green particles are the defects in the final ordered structure.

Fig. 6 shows the evolution of the two ensembles at $d = 1$. It was observed that at $\tau = 0.2$ the ensembles began to rotate around each other, and both ensembles appeared to expand to some extent. In addition, each ensemble had a chaotic structure. Because of the velocity fluctuation, the deformation of the circular shape of each ensemble starts, and the distance between the ensembles reduces. At a certain point, both ensembles begin to merge and subsequently form a single chaotic structure ($\tau = 1$). At $\tau = 4$, we can observe that the ensemble was quite ordered; however, there is a single particle (blue color) orbiting around the large ensemble. Eventually, the single particle merge with the ordered ensemble leads to the formation of a chaotic ensemble. The disordered ensemble eventually becomes a single rotating ordered structure around $\tau = 10$. The structure continued to expand until the repulsive forces between the particles diminished. At a time step of $\tau = 10000$, the panel indicates that the system has formed a hexagonally ordered structure plotted with the Delaunay triangulation, where the black, green, and pink particles have six, seven, and five neighbors, respectively. The green and pink particles represent defects in the system. The same neighbor counts and colors were used in further calculations. Both ensembles merged quickly due to their small initial separation. It is surprising that there was no attractive force between the ensembles, and yet both ensembles merged. The trajectories for these two ensembles are shown in Fig. 7*a*, with the same initial number of rotation of the ensembles that follow a circular path and get merged once they are close enough to each other. In Fig. 7*b*, we can observe a fluctuation in the separation between the ensembles after their merging (from $\tau = 0.5$ to $\tau = 8$), which was caused by the chaotic ensemble. However, after a time delay of $\tau = 9$, the separation appears to be constant with time, which can be explained by the ordering in the ensemble. All particles in the ensemble rotated with the same angular velocity. The distribution of particles (red and blue) from each ensemble was fixed in the final single-ordered ensemble, as shown in Fig. 6 ($\tau = 1000$).

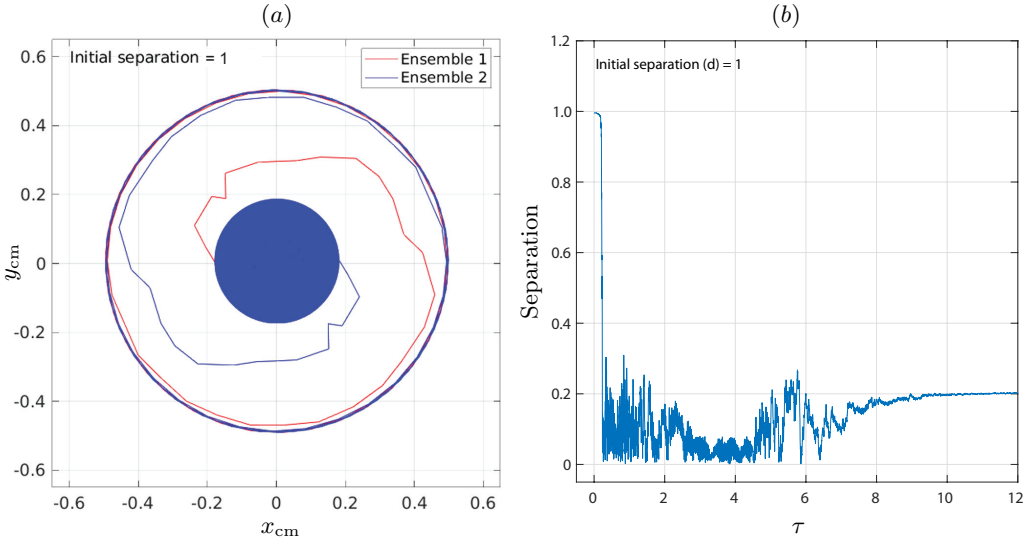

Fig. 7. (*a*) Trajectories of the center of mass of two ensembles, and (*b*) the separation between the center of mass of two ensembles with time as in Fig. 6, where $N = 50$ in each ensemble, the parameters $\lambda = 0.5$, $r_s = 0.05$, $d = 1$.

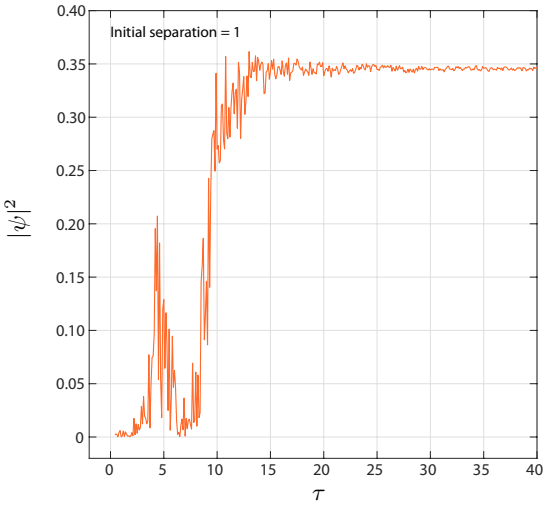

Fig. 8. The evolution of the hexatic order parameter for the initial separation $d = 1$, where $N = 50$ in each ensemble, the parameters $\lambda = 0.5$, $r_s = 0.05$.

The evolution of the hexatic order parameter $|\psi|^2$ for this system is shown in Fig. 8 according to the relation (I is the imaginary unit, N_{int} is the total number of internal particles, 'nn' is a nearest neighbor)

$$\psi_6(i) = \frac{1}{N_{\text{nn}}} \sum_{j \in \text{nn}} \exp\left(6I\vartheta_{ij}\right); \quad \psi = \frac{1}{N_{\text{int}}} \sum_{i=1}^{N_{\text{int}}} \psi_6(i), \tag{18}$$

which shows an increase in the hexagonal order parameter at $\tau = 4$ (Fig. 8) due to the formation of an ordered structure after merging. However, a single particle still rotates around the large-ordered ensemble, and when it merges with the large ensemble, there is a drop in the hexatic order parameter because the ensemble becomes chaotic (Fig. 6, $\tau = 6.5$). This indicates that the ensemble was sensitive to external perturbations. However, during evolution, this ensemble again forms an ordered structure, for which the hexatic order parameter remains constant, i.e. $|\psi|^2 \approx 3.5$ (Fig. 8, after $\tau = 25$). The hexatic order parameter for all cases was calculated for a single ensemble formed after the two ensembles merged.

Fig. 9 illustrates the behavior of the two ensembles when the initial distance between them increased to $d = 4$ for the same parameter values (λ and r_s). As shown, both ensembles rotated around each other for a certain period, and each ensemble ordered itself first. The distance between them decreases as time passes, and each ordered structure becomes deformed due to velocity fluctuations and eventually merges. After merging, the structure became chaotic. Subsequently, the structure began to form a single-ordered structure. This system takes a long time to reach an ordered state compared to the case of $d = 1$. In this case, $d = 4$ the final ordered structure does not expand even after a long wait; the reason could be the large initial separation between the two ensembles, where the particles no longer experience a repulsive force after the formation of a single ordered structure. Once the steady state achieved, a stable ordered structure was formed, and the total number of defects (pink and green particles) remained constant in both cases $d = 1$ and $d = 4$.

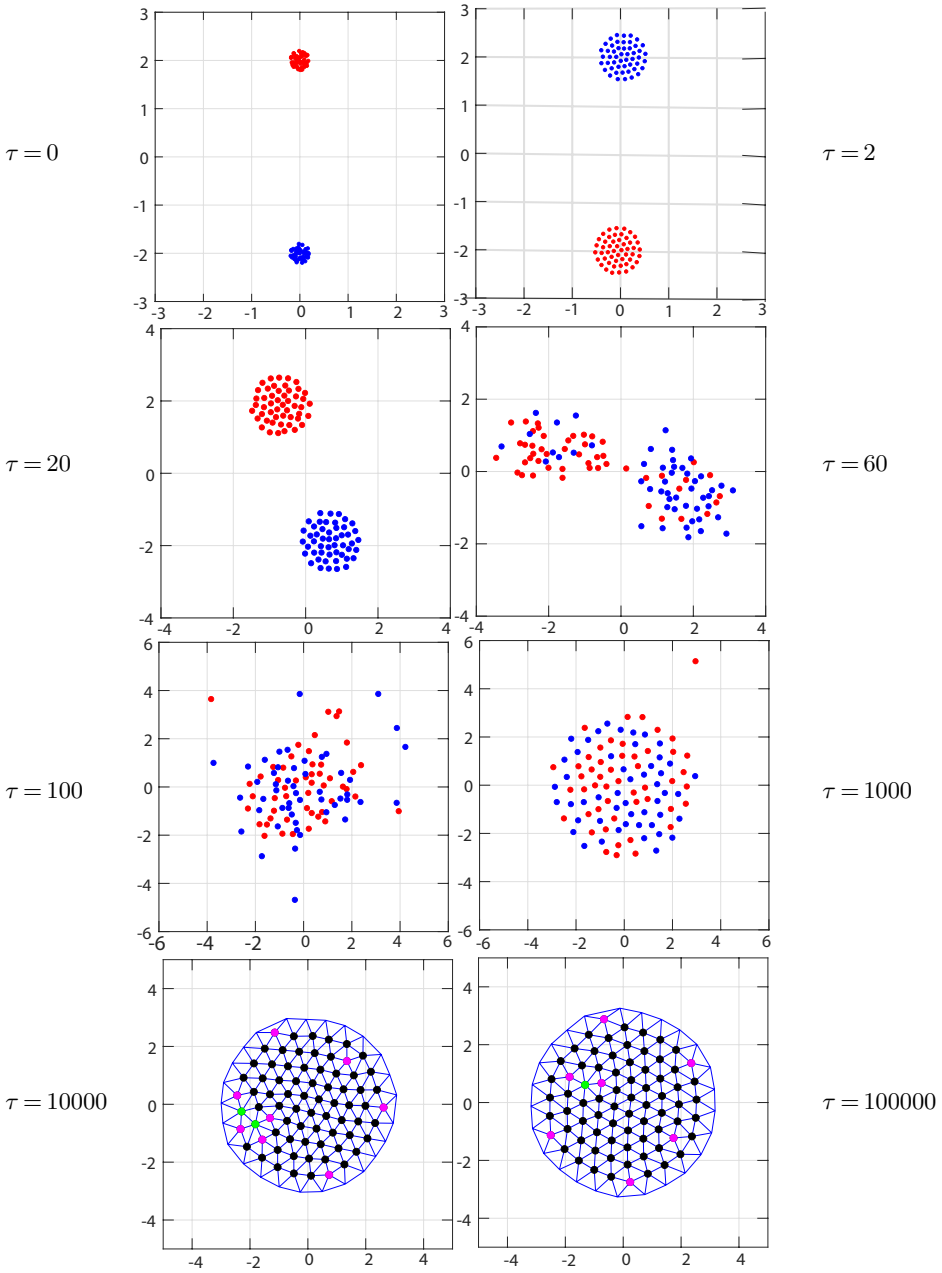

Fig. 9. Merging of two ensembles with time τ (red particles – ensemble one, blue particles – ensemble two), where the initial separation between the ensembles was $d = 4$, the parameters were $\lambda = 0.5$ and $r_s = 0.05$, the number of particles in each ensemble $N = 50$, and the total number of particles in the final single ensembles $N_T = 100$. The system evolves to a steady state, where it forms a hexagonally ordered structure, as shown by the Delaunay triangulation at $\tau = 100000$, where black particles have six neighbors, pink particles have five neighbors, and green particles have seven neighbors. The pink and green particles are the defects in the final ordered structure.

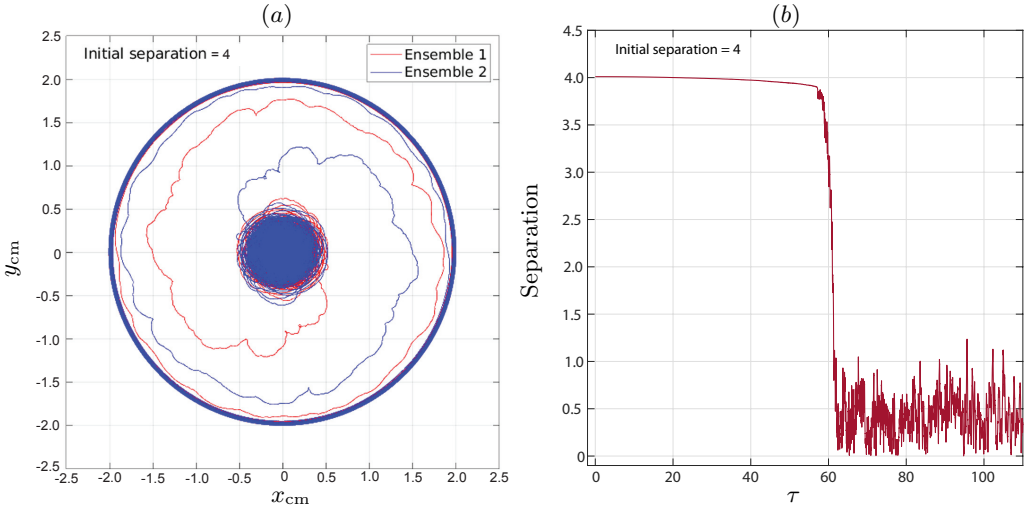

Fig. 10. (*a*) Trajectories of the centers of mass of ensembles with time, and (*b*) the separation of the center of mass of ensembles with time as in Fig. 9, where $N = 50$ in each ensemble, $\lambda = 0.5$, $r_s = 0.05$, $d = 4$.

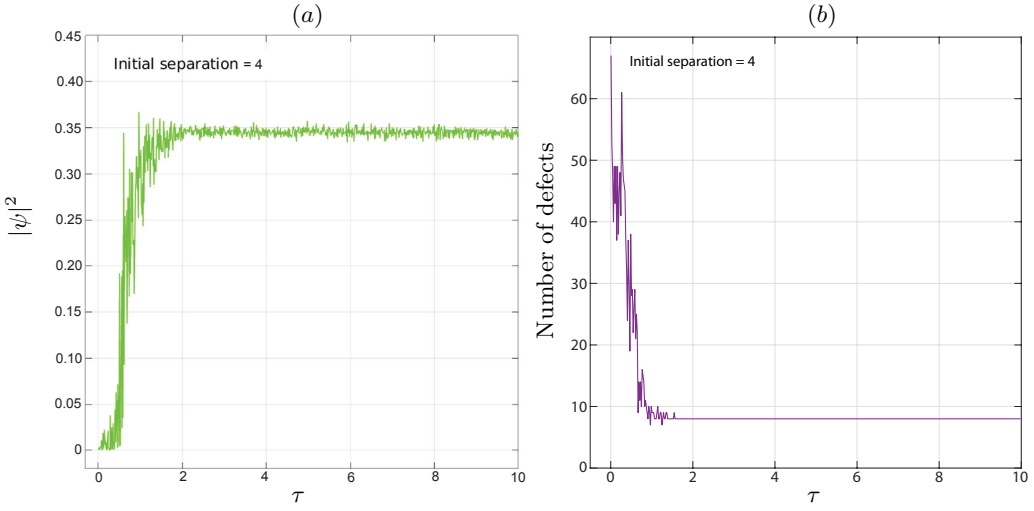

Fig. 11. (*a*) The evolution of the hexatic order parameter with time, and (*b*) the number of defects with time as in Fig. 9, where $N = 50$ in each ensemble, $\lambda = 0.5$, $r_s = 0.05$, $d = 4$.

Fig. 10*a* shows the trajectories of the center of mass of two ensemble for initial separation $d = 4$, and Fig. 10*b* shows the separation between the two ensemble over time, from which we can infer that as the separation between ensembles increases, the total number of rotations of the ensembles before merging increases, therefore, the separation is constant until $\tau = 40$. Once the ensembles are merged, there is a drop in separation, and, after merging, it fluctuates due to the chaotic structure. Fig. 11*a* shows the evolution of the hexatic order parameter with time for a system, where it approximate constant after the ordered structure formation. If wait sufficiently long, the final ensemble becomes an ordered structure with a fixed number of defects, as shown in Fig. 11*b* after time $\tau = 2 \times 10^4$.

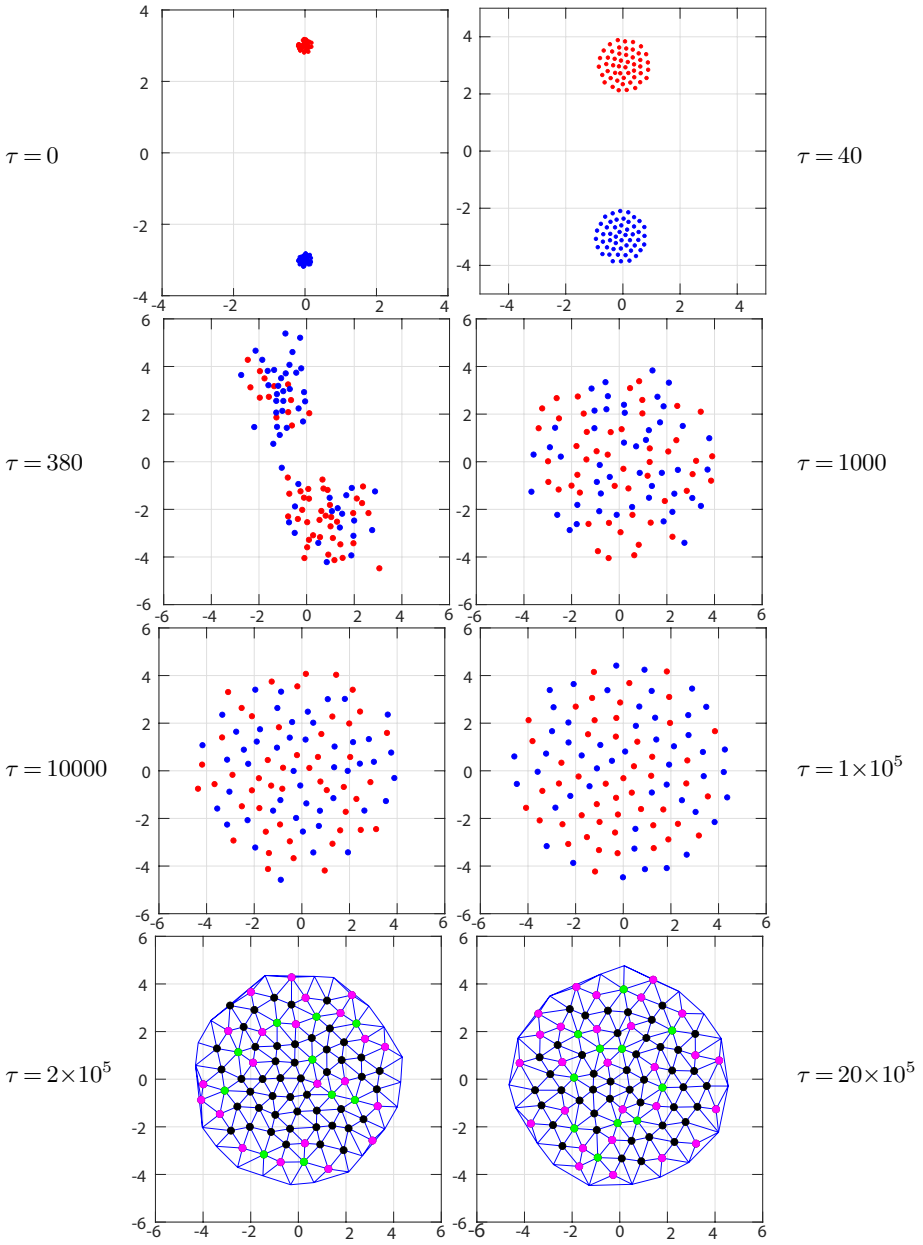

Fig. 12. Merging of two ensembles when the initial distance between them is $d = 6$; the parameters $\lambda = 0.5$, $r_s = 0.05$ for different time steps, where $N = 50$ in each ensemble and the total number of rotlets is $N_T = 100$.

Fig. 12 displays the two rotating ensembles with the initial separation between them being $d = 6$. As one can see, the two ensemble rotate around each other for some time, and the individual ensemble is ordered at $\tau = 32$. As the distance between them decreases, each ensemble deforms ($\tau = 380$) and eventually merges. Compared to the case when the initial separation was $d = 4$, this final single ensemble had more defects (pink and

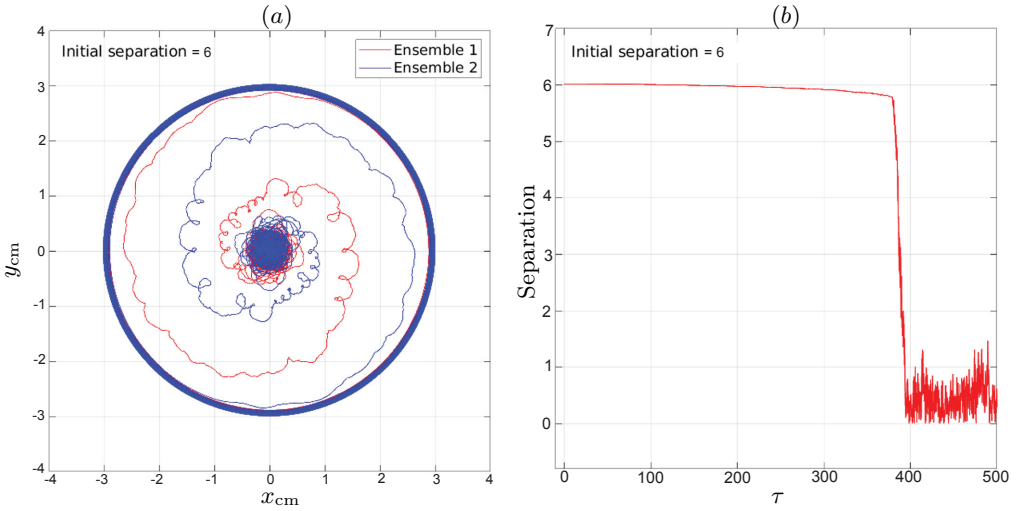

Fig. 13. (*a*) Trajectories of the centers of mass of ensembles with time; (*b*) the separation of the center of mass of ensembles with time as in Fig. 12, where $N = 50$, $\lambda = 0.5$, $r_s = 0.05$, $d = 6$.

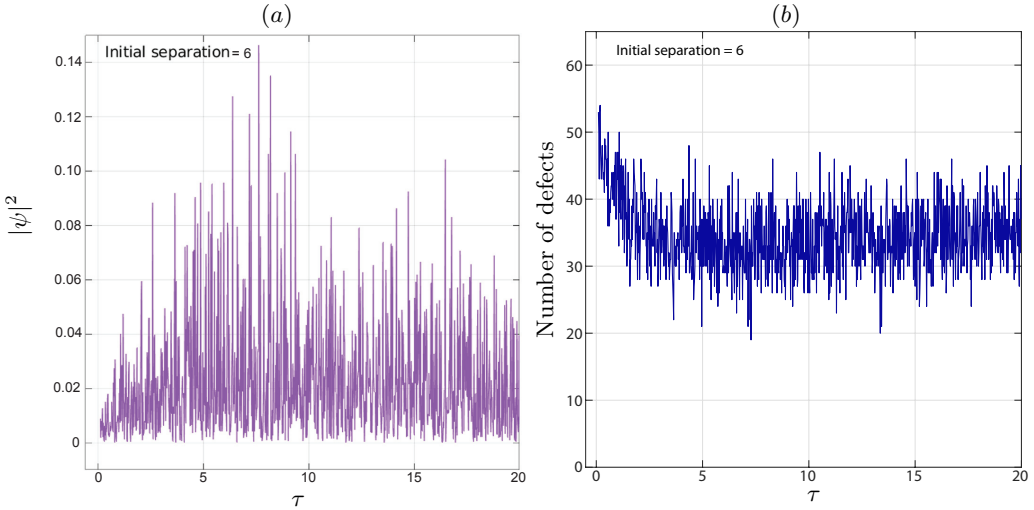

Fig. 14. (*a*) Hexagonal order parameter vs. time; (*b*) the total number of defects in the system with time, as in Fig. 12, where $N = 50$ in each ensemble, $\lambda = 0.5$, $r_s = 0.05$, $d = 6$.

green particles), and the structure did not achieve a hexagonal-order state, as observed in the case when the initial separation was $d = 1$ and $d = 4$. Despite waiting a long time for $\tau = 20 \times 10^5$, a final steady state has not yet been achieved. This can be explained as follows: because the initial separation between the two ensembles is quite large, it takes a long time to merge and to form a single ensemble. However, after merging, the distance between two particles is sufficiently large; therefore, the repulsive interaction between the particles diminishes, which keeps the final ensemble disordered, and has a greater number of defects.

The trajectories of the two ensembles are displayed in Fig. 13*a* that shows the two ensembles rotating for a long time $\tau = 300$ and coming close to each other gradually. After

merging, the ensembles had different trajectory structures due to the chaotic motion of the particles. The separation between the two ensembles, calculated from the center of mass of each ensemble over time, is presented in Fig. 13*b*, until $\tau = 250$ we can see that the separation is constant with time, where particles in each ensemble organize themselves into a hexagonally order structure due to the repulsive interaction, and also each ensemble expands to some extend. The decrease in separation after $\tau = 300$ indicates that each ensemble starts to deform and after merging fluctuates as both centers of mass of the ensembles move in a single chaotic ensemble. The variation in the hexagonal-order parameter with time is illustrated in Fig. 14*a*, which indicates that the final state is not hexagonally ordered, even at a later time. To confirm this, we checked at $\tau = 20 \times 10^5$ to determine whether there was any ordering in the final ensemble. However, even after a long wait, no hexatic-order structures were formed. The total number of defects in the system appeared to fluctuate by approximately 35, as shown in Fig. 14*b*. One explanation could be that as the ensembles are initially far from each other, the repulsive force between the particles vanishes after merging.

3. Conclusions.

In this paper, we discussed a theoretical model for two rotating ensembles of rotlets. When only hydrodynamic interactions between particles were considered, the two ensembles followed circular trajectories that were comparable to an approximate theoretical solution. When the repulsive force was considered along with the hydrodynamic interaction, the two rotating ensembles showed the merging and formation of an ordered structure even though there was no explicit attractive force between particles.

Acknowledgements. The authors acknowledge support by the Scientific Council of Latvia, grant No. lzp-2020/1-0149.

References

[1] B.A. Grzybowski, Ch.E. Wilmer, J. Kim, K.P. Browne and K.J.M. Bishop. Self-assembly: from crystals to cells. *Soft Matter*, vol. 5 (2009), pp. 1110–1128.

[2] A.P. Stikuts, R. Perzynski and A. Cēbers. Spontaneous order in ensembles of rotating magnetic droplets. *Journal of Magnetism and Magnetic Materials*, vol. 500 (2020), 166304.

[3] B.A. Grzybowski, H.A. Stone and G.M. Whitesides. Dynamic self-assembly of magnetized, millimetre-sized objects rotating at the liquid–air interface. *Letters to Nature*, vol. 405 (2000), pp. 1033–1036.

[4] B.A. Grzybowski, H.A. Stone and G.M. Whitesides. Dynamic self-assembly of magnetized, millimetre-sized objects rotating at a liquid–air interface. *In: Proc. the National Academy of Sciences (PNAS)*, vol. 99 (2002), pp. 4147–4151.

[5] W. Wang, J. Giltinan, S. Zakharchenko, M. Sitti. Dynamic and programmable self-assembly of micro-rafts at the air-water interface. *Science Advances*, vol. 3 (2017), e1602522.

[6] J. Yan, S.C. Bae and S. Granick. Rotating crystals of magnetic Janus colloids. *Soft Matter*, vol. 11 (2015), pp. 147–153.

[7] S. Kim and S.J. Karrila. Microhydrodynamics: Principles and selected applications. *Butterwoth-Heinemann*, (1991), p. 51.

[8] B. Shinde, R. Livanovics and A. Cēbers. Dynamics of rotlet's ensemble. *Journal of Magnetism and Magnetic Materials*, vol. 587 (2023), 171314.

Received 30.10.2023